Frequency Response of Multi-Phase Segmented *k*-Space Phase-Contrast

Jason A. Polzin, Richard Frayne, Thomas M. Grist, Charles A. Mistretta

A theoretical analysis of the temporal frequency response of multi-phase segmented *k*-space phase-contrast was developed. This includes the effects of both segment duration and the number of cardiac phases that are reconstructed. An increase in the number of views per segment and the corresponding increase in segment duration results in an increased smoothing or low-pass filtering of the time-resolved flow waveform. Reconstruction of all intermediate cardiac phases makes the Nyquist sampling frequency independent of the number of views per segment. This analysis was verified experimentally using a multi-phase phase-contrast segmented *k*-space MR pulse sequence. This sequence reconstructs all intermediate cardiac phases and uses fractional segments at the end of the cardiac cycle if an entire segment does not fit. The use of fractional segments increases the portion of the cardiac cycle over which data are acquired.

Key words: velocity mapping; cardiac gating; flow imaging.

INTRODUCTION

Cardiac gating can be used to acquire MR images at varying delays within the cardiac cycle relative to a physiological trigger. If each phase-encoding is acquired in a different heartbeat at the same delay, the resulting image will correspond to the anatomy at that point in the cardiac cycle. A drawback of such a technique is that the total imaging time can be quite long, taking as many heartbeats to acquire an image as there are k_y-lines in the acquisition. In this work, the acquisition of a single k_y-line is called a view. A compromise that reduces total imaging time is to segment the acquisition. In a cardiac-gated segmented *k*-space (1, 2) acquisition, *k*-space is divided up into segments, consisting of one or more views, each of which is acquired in a different cardiac cycle at the same trigger delay. These segments are then combined to form an image. Segmented *k*-space approaches can also be used in conjunction with phase-contrast to provide fast measurements of velocity and volume flow-rate. In segmented phase-contrast (SPC), data can be acquired in an interleaved or noninterleaved fashion. In an interleaved acquisition, all velocity-encodings for each view are acquired in the same cardiac cycle. In noninterleaved acquisitions, velocity-encoding for each view is done in separate cardiac cycles.

Recent work has demonstrated that SPC can provide fast and accurate volume flow-rate measurements. Initial results in work by Edelman *et al.*, (3) showed excellent correlation with a laser Doppler flow meter for phantom measurements of constant and mildly pulsatile flow using eight views per segment (VPS) and a noninterleaved acquisition. *In vivo* results obtained by this same group also demonstrated good correlation between segmented phase-contrast and cine phase-contrast for flow measured in the infrarenal abdominal aorta. Work by Keegan *et al.*, (4) compared flow measurements from a pulsatile flow phantom with frequency components less than 2 Hz using 1, 2, 3, and 4 VPS. The differences in the measured flow found by varying the number of VPS were very small. Li *et al.*, (5) found that SPC with up to five VPS correlates well with Doppler ultrasound measurements for a pulsatile waveform with significant temporal frequencies up to 2 Hz. Finally, Foo *et al.*, (6) have shown good correlation between SPC using two VPS and cine phase-contrast flow measurements in the descending aorta.

In this work, the accuracy of SPC measurements of time-varying (pulsatile) flow is examined. Specifically, the objective is to quantitate the temporal frequency response of SPC. In the process, two important results are demonstrated. (1) Temporal aliasing can be introduced during the reconstruction if an insufficient number of cardiac phases are generated; and (2) the temporal duration of each segment results in a low-pass filtering of the measured flow waveform.

THEORY

In a single cardiac-phase segmented *k*-space (1) acquisition, a segment of *k*-space is acquired centered about a specific delay from the cardiac trigger. Because each segment is acquired in a different cardiac cycle, the total acquisition takes as many heartbeats as there are segments in the acquisition, $N_{seg} = N_y/N_{vps}$, where N_y is the number of views in the acquisition, and N_{vps} is the number of views per segment. The resulting image depicts the state of the object at the time corresponding to the trigger delay, with some blurring or ghosting caused by motion during the segment duration (7).

A segmented *k*-space strategy can also be used for a multi-phase acquisition (2) in which each segment is continually repeated throughout the cardiac cycle. Each of these segments corresponds to an acquired cardiac phase. As in the single-phase case, it would seem that only one image need be reconstructed for each acquired

MRM 35:755–762 (1996)

From the Departments of Medical Physics (J.A.P., R.F., T.M.G., C.A.M.) and Radiology (R.F., T.M.G., C.A.M.), University of Wisconsin-Madison, Madison, Wisconsin.

Address correspondence to: Jason A. Polzin, G.E. Medical Systems, P.O. Box 414-W827, Milwaukee, WI 53201-0414.

Received July 26, 1995; revised November 30, 1995; accepted December 6, 1995.

This work was supported in part by National Institutes of Health Grant R01 HL52747-01A1 and a grant from the Whitaker Foundation. J.A.P. was supported by National Institutes of Health NRSA Grant CA09206-01. R.F. is supported by a Heart and Stroke Foundation of Canada Fellowship. T.M.G. is supported in part by National Institutes of Health Grant K08 HL02848.

0740-3194/96 $3.00

Copyright © 1996 by Williams & Wilkins
All rights of reproduction in any form reserved.

phase in the cardiac cycle; however, as shown in Fig. 1, for the case of interleaved two-point velocity-encoding with four views per segment, it is apparent that a unique image or cardiac phase can be reconstructed for nearly every view within the R-R interval. This was first noted by Foo *et al.*, (6) where they called the reconstruction of intermediate cardiac phases, "view-sharing." In that work, only a single intermediate cardiac phase was reconstructed for each pair of adjacent acquired phases. Using the general approach of reconstruction of all intermediate cardiac phases, it is not necessary to acquire an integer number of segments within each cardiac cycle. This is important when the duration of the segments becomes long relative to the cardiac cycle duration where only a small number of segments will fit within each cycle. This is shown in Fig. 1 where three views from a fifth acquired phase are acquired, allowing three additional cardiac phases to be reconstructed.

For interleaved SPC, the segment duration is $T_s = N_{vps} N_v TR$, where N_v is the number of interleaved velocity-encodings, and TR is the sequence repetition time. The time required to acquire all velocity-encodings with the same phase-encoding is $T_a = N_v TR$. Conventionally, one cardiac phase is reconstructed for each acquired phase (2, 5). The total number of reconstructed cardiac phases, N_{rec}, is then equal to the number of acquired cardiac phases, N_{acq}, where $N_{acq} = \text{int}(T_{HB}/T_s)$, T_{HB} is the cardiac cycle duration, and int is the integer component. The view-sharing proposed by Foo *et al.* increases the number of cardiac phases by reconstructing an intermediate phase from adjacent acquired phases for a total of $N_{rec} = 2N_{acq} - 1$ phases. The -1 is necessary because views are not shared between acquired cardiac phase 1 and N_{acq}. Reconstruction of all intermediate cardiac phases results in $N_{rec} = N_{vps}(N_{acq} - 1) + 1$ phases. If fractional segments are used, this becomes, $N_{rec} = T_{HB}/T_a - N_{vps} + 1$. Again, as in the single intermediate cardiac phase case, the number of reconstructed phases is reduced because views are not shared between acquired phase 1 and N_{acq}.

For SPC and cardiac gated acquisitions in general, two types of gating are possible. Historically these have been defined as retrospective (8, 9) and prospective (10) gating. In the most general terms, in this work prospective is used to mean any acquisition that is synchronous with the cardiac trigger, either ECG or peripheral. Any asynchronous acquisition, in which synchronizing with the cardiac trigger is done during reconstruction, is called retrospective. For example CINE-PC (General Electric Medical Systems, Milwaukee, WI) (11) is retrospective, even though the view number is updated after detection of the cardiac trigger, because data are interpolated during reconstruction. In general, constant TR (6) acquisitions are retrospective techniques because of the timing jitter of up to one TR that is present between the start of data acquisition and the cardiac trigger. This jitter is removed by data interpolation during reconstruction.

If an SPC acquisition is used to measure time-varying flow, the measured flow waveform will be a smoothed version of the actual flow waveform. This smoothing is a result of averaging flow over the segment. The longer the segment duration, the smoother the measured flow waveform will be. For a more quantitative approach to the frequency response of constant TR SPC, a Fourier analysis (12) is necessary. This is shown schematically in Fig. 2a for an acquisition with two VPS. The time domain analysis is shown on the left, and the frequency domain analysis is shown on the right. Here the imaging process has been broken into two steps: data acquisition and data reconstruction. The data acquisition step consists of sampling during data acquisition (primary sampling). The reconstruction has been separated into two additional steps: interpolation and sampling during reconstruction (resampling), although in practice during reconstruction, the interpolation and resampling steps are combined. Images corresponding to each desired trigger delay are reconstructed by performing the interpolation at only specific delay times.

In an MR experiment, data is acquired at discrete times, separated by TR. In interleaved phase-contrast, two or four consecutive velocity-encoded acquisitions are required for each phase-encoding to obtain flow information in either one or all three directions ($N_v = 2$ or $N_v = 4$) (13). A continuous-time flow waveform would then be sampled every $T_a = N_v TR$ with each new phase-encoding value as depicted in steps i–iii of Fig. 2a. Step i shows the continuous flow waveform in both the time and temporal frequency domains. In SPC, even though

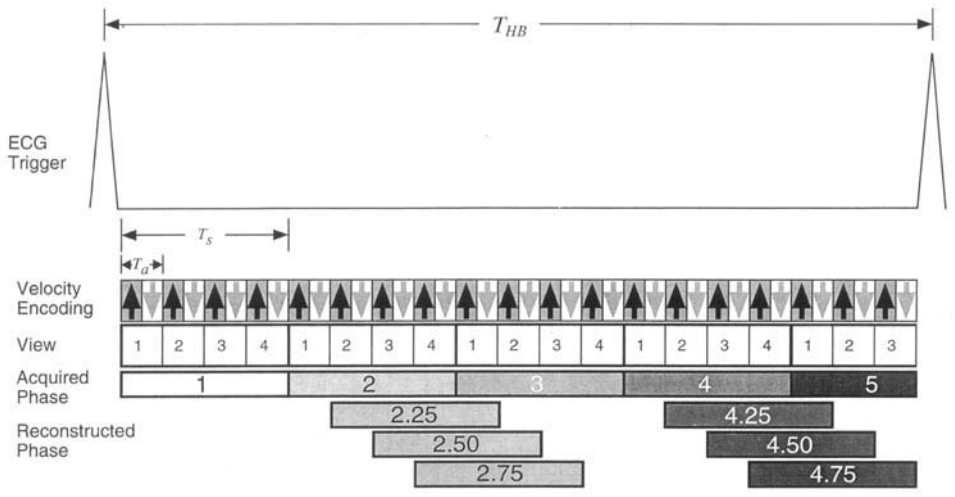

FIG. 1. Diagram depicting a single cardiac cycle from a four VPS ($N_{vps} = 4$) interleaved two-point ($N_v = 2$) acquisition. Reconstruction of additional intermediate cardiac phases is depicted. A fractional segment is also shown in which only three of the four views within the fifth acquired phase are acquired. This allows an additional three cardiac phases to be reconstructed. Cardiac cycle duration, T_{HB}, segment duration, T_s, and velocity-encoding acquisition duration, T_a, are all labeled.

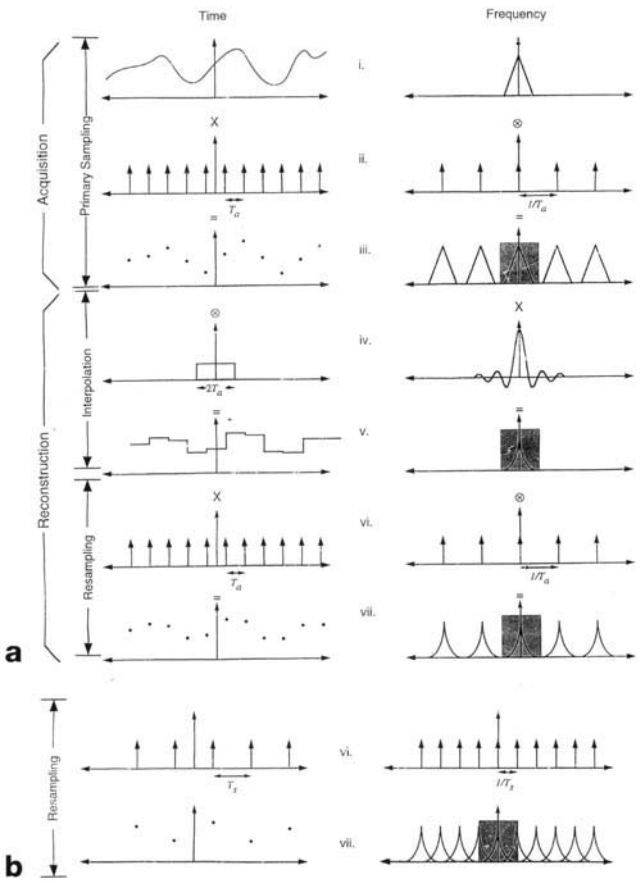

FIG. 2. Diagram showing the time and temporal frequency domain analysis of segmented phase-contrast for $N_{vps} = 2$. In Fig. 2a this is divided up into two parts: data acquisition, which includes primary sampling; and reconstruction, which includes interpolation and resampling. In sampling during acquisition, the phase-encoded data are acquired at intervals of T_a, hence the waveform is sampled every T_a. In the interpolation step, the nearest N_{vps} phase-encodings are grouped to form an image at that point in the cardiac cycle. In the resampling during reconstruction step, the sampling rate is determined by the number of cardiac phases that are reconstructed. In Fig. 2a, because all phases are reconstructed, sampling is every T_a, resulting in a frequency spectrum that is replicated every $1/T_a$. In Fig. 2b, no intermediate phases are reconstructed, corresponding to sampling every T_s. This results in a replication of the frequency spectrum $1/T_s$. In this case, aliasing occurs when there is overlap of the spectra.

each data sample corresponds to a different view, it still contains information about the entire object, and hence the temporally varying waveform. This sampling in the time domain corresponds to multiplication of the continuous time function by a comb function with spacing T_a, as shown in steps ii and iii. In the frequency domain, this is equivalent to convolution of the original frequency spectrum with a comb function having spacing $1/T_a$ (14). Temporal aliasing of the flow waveform can occur if the sampled temporal waveform has frequency components greater than the Nyquist frequency of the data acquisition sampling rate, $f_N = 1/2T_a$. For two velocity-encodings and a *TR* of 16 ms, the Nyquist sampling frequency is 16 Hz, which includes all but the highest harmonics found *in vivo* (15). The final sampled waveform is shown in step iii.

Because a retrospective acquisition is asynchronous with respect to the cardiac trigger, the sampled data must be interpolated during the reconstruction to generate images corresponding to the different cardiac trigger delays (8, 9, 11). In SPC, this interpolation step is equivalent to the grouping together of the nearest N_{vps} views at each point in time from each cardiac cycle to generate an image. In the interpolation step, a continuous representation of the sampled waveform is obtained by convolving it with an interpolation kernel. For example with CINE-PC (12) a linear interpolation kernel is used. For SPC, the appropriate kernel must be wide enough to group together all views within the segment (T_s), and give uniform weighting to each sample within this range. Nearest-neighbor interpolation (NNI), where the interpolating function has a uniform weighting over a duration T_s, is the appropriate kernel for this analysis. This is shown in step iv of Fig. 2a for a segment duration of $T_s = 2T_a$. The resulting continuous function is represented in step v. In the frequency domain, convolution with the NNI kernel is the same as multiplication of the replicated frequency spectrum by the Fourier transform of this kernel. The Fourier transform of the NNI kernel of width T_s is a sinc function with zero-crossings at $1/T_s$ (14). Hence, the larger the number of views per segment, the sharper the fall-off of the sinc function, and greater the suppression of high temporal frequency information. Mathematically, this is equivalent to multiplication of the frequency spectrum by the frequency domain transfer function for $N_{vps} = m$,

$$H_m(f) = \mathrm{sinc}(N_v m\, f\, TR) = \frac{\sin(\pi\, N_v\, m\, f\, TR)}{\pi\, N_v m\, f\, TR}. \qquad [1]$$

After interpolation, the resulting continuous function must be resampled to reconstruct images corresponding to various trigger delays. The number of images to reconstruct determines the time between samples during reconstruction, T'. Segmented phase-contrast reconstruction with no intermediate cardiac phases results in an image reconstructed every $T' = T_s$ with a corresponding Nyquist frequency of $f'_N = 1/(2T_s)$. View-sharing as proposed by Foo *et al.*, (6) reduces the sampling period by a factor of two ($T' = T_s/2$) and has a corresponding Nyquist frequency, $f'_N = 1/T_s$.

Using a sampling period during reconstruction $T' = T_a$, i.e., reconstructing all intermediate phases, the resampling rate is the same as that of the initial sampling during acquisition. Hence, by reconstructing all possible cardiac phases, the Nyquist frequency of the resampling during reconstruction is matched to the Nyquist frequency of the initial sampling during data acquisition and is equal to $f'_N = 1/(2T_a)$. Any further increase in the number of cardiac phases to be reconstructed will not help to resolve higher temporal frequencies because they have already been aliased in the data acquisition sampling step. This is shown in step vi and vii of Fig. 2a where the interpolated waveform is multiplied by a comb function with spacing T_a in the time domain or convolved with a comb function with spacing $1/T_a$ in the frequency domain. The final discrete function is a low-pass filtered version of that shown in step iii.

Figure 2b depicts how aliasing can be introduced during reconstruction if the resampling Nyquist rate, $f'_N < 1/T_a$, is less than the Nyquist sampling rate during acquisition. In this example (Fig. 2b), no intermediate cardiac phases are reconstructed, corresponding to multiplication by a comb function with spacing T_s. Hence, after resampling during reconstruction, frequencies greater than $1/(2T_s)$ will overlap, causing lower frequencies to be misrepresented. An important point that should be kept in mind with respect to the consequences of aliasing caused by resampling is that aliasing does not result in a corruption of each measured data point. Rather, the insufficient number of data points, i.e., insufficient sampling, will result in a misrepresentation of intermediate values if the original continuous waveform is estimated from the resampled waveform using interpolation.

The above analysis assumes that data acquisition is gated retrospectively (i.e., data acquisition is not synchronized with the cardiac trigger) and that some type of interpolation, in this case NNI, is needed to "synchronize" the data with specific times in the cardiac cycle. In the actual reconstruction, whether prospective or retrospective, the reconstruction process is the same. An image corresponding to the desired trigger delay is reconstructed by grouping together the N_{vps} views in each cardiac cycle nearest that delay. This ensures that all of the necessary views are used in the reconstruction.

In prospectively gated SPC in which data acquisition is synchronized with the cardiac trigger, all velocity- and phase-encodings are acquired at discrete points in the cardiac cycle. The frequency response of prospectively gated phase-contrast for the case of one view per segment has been previously reported (16). For greater than one view per segment, the analysis is greatly simplified if it is assumed that all encodings contribute equally, and the measured flow is the mean flow over all of these discrete points within a segment duration, T_s. A balanced two-point acquisition (17) results in equal contribution from all of the velocity-encodings. For a four-point method, a balanced Hadamard (18) encoding scheme would also result in equal contribution from each of the velocity-encodings. The frequency response is then the Fourier transform of a discrete summation across all acquisitions within the segment. In digital signal processing, this is commonly referred to as the discrete averaging filter (19). The frequency response is,

$$|H_{ni}^{pro}(f)| = \frac{\sin(\pi N_v m f TR)}{N_v m \sin(\pi f TR)}. \quad [2]$$

For all frequencies such that $f < 1/(\pi TR)$, the retrospective and prospective frequency responses are nearly identical.

The theory developed in this work only strictly applies to a vessel with a uniform k-space distribution or equivalently a delta function in the image domain. In this case, each view contributes equally to the measured flow which would then be equal to the mean flow rate over the segment duration. For vessels that differ significantly from a delta function, there may be some variation from the predicted frequency response given by Eq. [1] or [2]. This would be caused by the nonuniform weighting over the segment duration, which results in a measured flow rate that deviates from the mean flow rate over the segment duration. The amount of deviation from theory would also depend on the view order used to acquire data. In a segmented-interleaved view ordering (2, 5) in which all of k-space is traversed in each segment, a number of central k_y-lines equal to the number of segments, N_{seg}, is acquired at the same point in each segment. This results in the measured flow being heavily weighted toward this point and hence deviating from the mean flow over the segment. In addition, interleaved strategies do not lend themselves well to reconstruction of additional intermediate cardiac phases because the data are so heavily weighted toward one point in the segment. In sequential encoding strategies (6), neighboring views are acquired in each segment and measured flow is equal to the mean flow for vessels of even moderate size (20).

METHODS

The frequency response of segmented phase-contrast was validated experimentally using a computer-controlled flow pump (Quest Imaging, London, ON) (21). The MR data were acquired using a 1.5 T Signa MR scanner (G.E. Medical Systems) with a modified version of FASTCARD-PC (6).

FASTCARD uses a constant *TR* RF excitation, multiphase segmented k-space acquisition to acquire data over a large fraction of the cardiac cycle. Even when data are not being acquired, a slice-selective RF pulse is still applied every *TR* to keep the longitudinal magnetization in a steady state. This eliminates the "flash" artifact (9) present with other non-constant *TR*-gated acquisitions that image over only a portion of the cardiac cycle and allow spins to relax during the portion of the cardiac cycle not used for imaging. The constant *TR*, as described previously, also introduces "jitter" into the start of the acquisition with respect to the cardiac trigger. By our strict definition of retrospective and prospective, FASTCARD uses a retrospective gating scheme, and therefore has a frequency response that is described by the retrospective analysis (Eq. [1]).

FASTCARD was modified to reconstruct all intermediate phases. A cardiac phase was reconstructed for every set (either two or four) of velocity-encoded acquisitions in the cardiac cycle. Fractional segments were used at the end of the cardiac cycle to increase the portion of the cardiac interval over which data were acquired. The view order used in this work was an alternating centric acquisition in which the central N_{vps} views, were acquired in the first cardiac cycle and in subsequent cycles the $N_{vps}/2$ views closest to and on either side of the central k_y view were acquired. For example with N_{vps} = 8, and 128 phase-encodings, the acquisition would be as follows: HB #1, 61–68; HB #2, 57–60 and 69–72; . . .; HB #16, 1–4 and 125–128, where HB is the heartbeat. This encoding strategy is very similar to a sequential acquisition with the addition that positive and negative spatial frequencies are acquired in the same segment.

The computer-controlled pump was used to drive blood-mimicking fluid through 6.35-mm inner diameter

tubing. Raised cosine waveforms, consisting of a cosine flow waveform of a given frequency with an additional constant offset, with frequencies ranging from 1 to 5 Hz were used to validate the frequency response. Raised cosines were used so that the pressure in the tubing was always positive, which resulted in improved flow waveforms. Data were then acquired at each frequency for N_{vps} = 1, 2, 4, 6, and 8. Pulse sequence parameters were matrix size = 256 × 256, field of view (FOV) = 20 cm, slice thickness = 0.5 cm, velocity-encoding = 100 cm/s, balanced two-point encoding, *TR* = 18.4 ms, tip angle = 30°, and four signal averages.

The resulting waveforms were then fitted using Levenberg–Marquardt nonlinear least squares (22) to a function of the form y(t) = a + b*cos(c*t+d). The frequency term, c, was noted for discrepancies from the expected temporal frequency of the measured waveform. In addition, for each set of frequencies, the phase term, d, was used to determine the polarity of the fitted amplitude. Finally, the amplitude term, b, was normalized to the amplitude for the one view per segment acquisition to determine the frequency response relative to one view per segment. The functional form of the relative transfer function is obtained by taking the ratio of Eq. [1] for *m* VPS to that for one VPS,

$$H'_m(f) = \frac{H_m(f)}{H_1(f)} = \frac{\sin(\pi N_v m f TR)}{m \sin(\pi N_v f TR)} \quad [3]$$

The effects of sampling during reconstruction (resampling) were analyzed for eight views per segment for 1, 2, and 5 Hz waveforms. Resampling was done at $T' = T_a$ (reconstruct all intermediate phases), $T' = T_s/2$ (reconstruct one intermediate phase), and $T' = T_s$ (reconstruct one phase per acquired phase). The waveforms were then fit to a cosine function as described previously and the measured frequency was compared with the expected frequency.

In vivo results were also obtained using the modified version of FASTCARD-PC in the descending aorta of a volunteer. Images were acquired using both one and four VPS for comparison. Imaging parameters were matrix size = 256 × 128, FOV = 24 cm, slice thickness = 1 cm, velocity-encoding = 150 cm/s, balanced two-point encoding, *TR* = 16.2 ms, tip angle = 30°, torso phased-array coil (G.E. Medical Systems), and one signal average. Each acquisition was repeated four times to estimate the reproducibility. All intermediate cardiac phases were reconstructed.

RESULTS

Phantom Experiments—Frequency Response

Figure 3 shows a comparison between the measured flow for one and eight VPS at 5 Hz. The measured amplitude of modulation at one VPS was 3.41 ± 0.10 ml/s at a frequency of 5.00 ± 0.02 Hz, with a relative phase of 58.1 ± 3.4°. The measured amplitude at eight views per segment was 0.71 ± 0.05 ml/s at a frequency of 5.05 ± 0.05 Hz with a relative phase of −109.5 ± 9.6°. The phase shift between the two acquisitions is 167.6 ± 10.2°. The

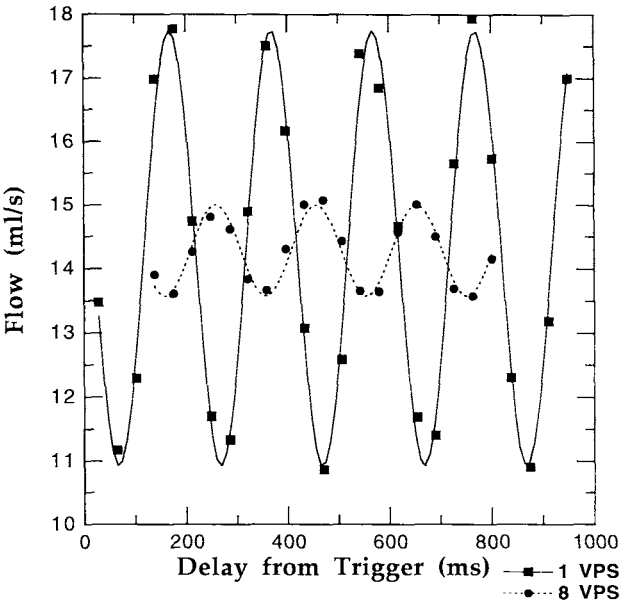

FIG. 3. Comparison of the measured and fitted flow waveforms for one and eight VPS at 5 Hz. The eight VPS amplitude of modulation is much smaller, as well as being inverted, than the one VPS modulation.

measured waveform using eight VPS is considerably dampened as well as being inverted in phase relative to the one VPS measured waveform.

Figure 4 shows the measured and theoretical frequency response from Eq. [3] for 2, 4, 6, and 8 VPS normalized to the one VPS response. Error bars represent one standard

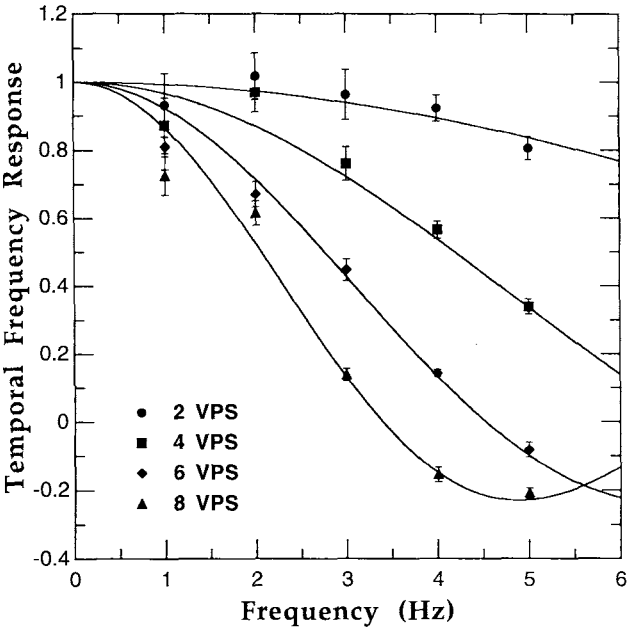

FIG. 4. Measured and theoretical frequency response curves for 2, 4, 6, and 8 VPS relative to one VPS. Balanced interleaved two-point velocity-encoding with a *TR* of 18.4 ms was used. Measured values are plotted as symbols with error bars representing one standard error. Theoretical responses are plotted as lines. Notice the inversion of frequency response that occurs at higher frequencies for six and eight views per segment.

error and were calculated from the diagonal elements of the covariance matrix resulting from the fit (22). The expected inversion of the frequency response from the negative lobes of the sinc function for six VPS at frequencies >4.5 Hz and for eight VPS at frequencies >3.4 Hz is supported by the experimental results.

Phantom Experiments—Sampling during Reconstruction

The effects of sampling during reconstruction (resampling) are shown in Fig. 5 for 1, 2, and 5 Hz waveforms at eight views per segment for $T' = T_s$, $T_s/2$, and T_a. In each case, the calculated expected frequency, f_{exp}, and the measured frequency, f_{meas}, are included. For frequencies less than f'_N, f_{exp} is the same as the input waveform frequency. However, for frequencies greater than f'_N, f_{exp} will not accurately represent the input waveform frequency and will be aliased.

For all resampling periods, the 1 Hz waveform was adequately sampled. For $T' = T_a$, and $T_s/2$ the 2 Hz waveform was also adequately sampled. However for $T' = T_s$, the Nyquist frequency caused by resampling is 1.7 Hz and the 2 Hz waveform should alias to 1.4 Hz. This is consistent with the measured waveform frequency of 1.27 Hz. The 5 Hz waveform was only adequately sampled for $T' = T_a$. Resampling at $T' = T_s/2$ ($f'_N = 3.4$ Hz) results in a measured aliased frequency of 1.68 ± 0.24 Hz compared with the expected aliased frequency of 1.79 Hz. Resampling at $T' = T_s$ results in measured and expected aliased frequencies of 1.60 and 1.85 Hz, respectively.

In Vivo Experiment

The results from the *in vivo* experiments are shown in Fig. 6 with error bars corresponding to one standard error. Peak systolic flow is underestimated using four VPS compared with one VPS because of more severe low-pass filtering. In this case, the measured peak flow was 239.0 ± 10.3 ml/s, compared with the measured peak flow of 275.4 ± 11.5 ml/s for one view per segment. The results of an unpaired t test comparison of the peak flows gave a significance of >95% that the measurement differences were not just because of measurement error. The mean flow over the cardiac cycle for four and one VPS was 86.0 ± 2.2 ml/s and 89.9 ± 2.7 ml/s, respectively. The differences were not significant using an unpaired t test. The mean flow measurements should be

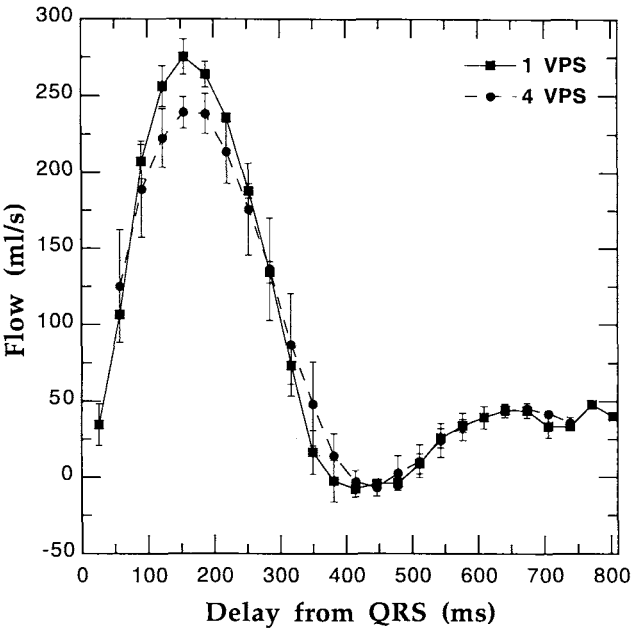

FIG. 6. *In vivo* results comparing the response of one view per segment and four views per segment in the descending aorta. Results shown are the average of four measurements with error bars corresponding to one standard error. Note that the systolic peak is reduced for the four VPS acquisition because of the reduction in contribution from higher temporal frequencies.

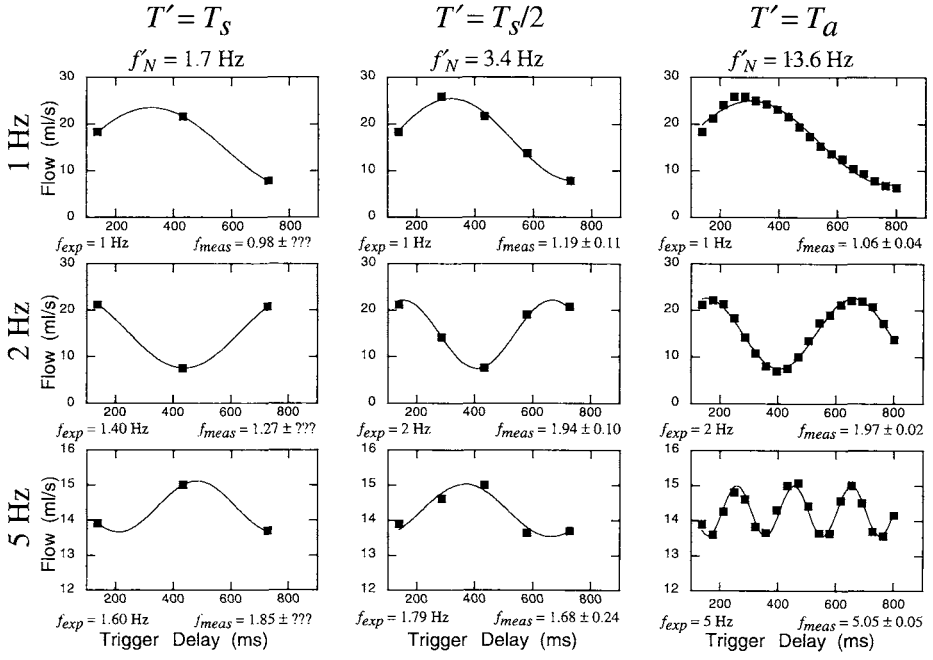

FIG. 5. Comparison of measured and expected frequencies for 1, 2, and 5 Hz waveforms for resampling intervals of $T' = T_s$, $T_s/2$, and T_a with Nyquist frequencies of 1.7, 3.4, and 13.6 Hz, respectively. Expected frequency, f_{exp}, and measured frequency, f_{meas}, are shown. For resampling at $T' = T_s$, the error in f_{meas} is undefined because of the limited number of points used in the fitting. The 1 Hz waveform is sampled adequately for all resampling intervals. The 2 Hz waveform is aliased at $T' = T_s$, and the 5 Hz waveform is aliased at $T' = T_s/2$, and T_s.

independent of segment duration because the 0 Hz (DC) response is unity for all number of VPS.

DISCUSSION

As described in the theory section, view order and vessel size may be of importance in determining the frequency response. In this work, the frequency response theory holds if the measured flow is equal to the mean flow over the segment duration. This will be true if the object has a uniform *k*-space distribution or equivalently is a delta function in the image domain. However, in the experiment performed for this work, the imaged tubing was approximately eight pixels in diameter and so differed significantly from a delta function. In this case, roughly the cental 32 views contribute to the measured flow (23). This measured flow will be dominated by the central *k*-space segment, which for alternating centric view ordering is approximately equal to the mean flow over the segment duration.

In alternating centric view ordering, the first segment contains the central N_{vps} views. This is also the case for sequential view ordering with an offset of $N_{vps}/2$. For this reason, it is expected that the measured frequency response of alternating centric or the more commonly used sequential-offset view ordering would be very similar.

In the limit of a vessel, which encompasses the entire imaging FOV, the *k*-space data will consist of a single point at the origin. Because the origin is only sampled in one cardiac cycle and then only once per segment, frequencies beyond $f_N = 1/(2T_s)$ will not be resolved. However, because only the central k_y-line contributes to measured flow, frequency response up to f_N would be similar to the response for one VPS.

If a noninterleaved velocity-encoding strategy is used, the frequency response is independent of the number of velocity-encodings used and segment duration depends only on the number of views per segment. However, the number of views per segment must be increased by a factor equal to the number of velocity-encodings to preserve the same total acquisition time. In other words, for the same total acquisition time, the segment duration is the same for interleaved or noninterleaved SPC. Neglecting cardiac cycle variability, if the imaging time is kept the same for an interleaved and a noninterleaved acquisition, the frequency response will remain the same unless the variation in *k*-space weighting is significant.

For non-breath-hold applications, the reduction in imaging time afforded by acquiring more than one view per segment can be traded for increased signal averaging. This would help to improve signal-to-noise as well as provide a pseudo-gating (24) effect in regions where respiration is a problem but breath-holds are not feasible.

For two views per segment, the acquisition can be completed in half the time needed for a conventional prospectively or retrospectively gated acquisition. The zero-crossing of the two views per segment frequency response, $f = 1/(2T_a)$, is matched to the Nyquist frequency, f_N, of the data acquisition. The 50% reduction in total imaging time comes at the expense of only a small degradation in frequency response. The response relative to one view per segment from Eq. [3] is $H'_2 = \cos(\pi N_v TR f)$, which results in a 3 dB attenuation at a frequency of $\frac{2}{3} f_N$.

Reconstructing only one intermediate phase per pair of acquired phases, is sufficient for most *in vivo* applications in which the flow waveform is band limited to $1/T_s$. This resolves all frequencies within the central lobe of the sinc temporal frequency response. Frequencies beyond the main lobe can be resolved but at the expense of additional reconstruction time and storage space.

The generality of this analysis implies that interpolation schemes other than NNI could be used. Linear interpolation would have a sinc^2 frequency response with a zero-crossing at $1/T_s$. Those frequencies less than the zero-crossing frequency would be more severely attenuated than in the case of NNI interpolation. However, frequencies greater than the zero-crossing would also be more severely attenuated, reducing the effects of aliasing introduced during reconstruction from these side-lobes.

The available imaging time is the amount of time in the cardiac cycle over which data can be acquired. Typically, this time is set to be less than the time between ECG triggers to account for any minor arrhythmias that may occur during the acquisition. However, if a major arrhythmia occurs, which reduces the cardiac cycle duration to be less than the available imaging time, data will be acquired after detection of the ECG trigger and will be corrupted. The use of fractional segments does not correct for this but rather insures that the entire available imaging time is used.

For the phantom frequency response experiments, the time between simulated cardiac triggers was 1000 ms. The available imaging time was set to 96% of the cardiac cycle allowing 4% for arrhythmias. Since the cardiac cycle was completely periodic, this actually was not necessary. This resulted in an available imaging time of 960 ms. For a *TR* of 18.4 ms, that is enough time for 52 acquisitions or 26 velocity-encoded pairs in the cardiac interval. Thus, only three *complete* segments at eight VPS would fit into the available imaging time for a total of 24 velocity-encoded pairs. Data can be acquired over more of the total available imaging time by using fractional segments. For the phantom experiments, the first two views from a fourth segment were acquired for a total of 26 velocity-encoded pairs. This increased the amount of time in the cardiac cycle over which data was acquired by 74 ms. For a more extreme example, if there were 1100 ms of available imaging time within the cardiac interval and data were acquired using eight VPS, only three complete segments would fit within this interval. The use of fractional segments would have allowed seven additional velocity-encoded pairs corresponding to an additional 258 ms of imaging time and the reconstruction of an additional seven cardiac phases.

CONCLUSION

Segmented *k*-space phase-contrast has become a common method for acquiring fast cardiac-gated data within a breath-hold (3–6). The reduction in total imaging time with SPC results in an attenuation of high temporal frequencies. In this work, this reduction in information has been quantified. In addition, some rationale for recon-

struction of additional cardiac phases beyond one per acquired phase has been given.

It has been shown that data reconstruction in SPC can be modeled as (1) interpolation, which results in low-pass filtering of the flow waveform by a sinc function with zero-crossings at $1/T_s$, and (2) resampling, which can introduce temporal aliasing. The low-pass filtering effect is inherent to the technique and so is unrecoverable. By reconstructing all intermediate cardiac phases, the reconstruction Nyquist frequency is matched with the data acquisition Nyquist frequency and *no additional aliasing* is introduced during the reconstruction process. The aliasing frequency is then only dependent on T_a and is independent of segment duration and thus the number of views per segment. An additional advantage of reconstruction of all intermediate cardiac phases is that fractional segments can be used to extend the portion of the cardiac cycle over which data are acquired.

REFERENCES

1. R. R. Edelman, B. Wallner, A. Singer, D. J. Atkinson, S. Saini, Segmented turboFLASH: method for breath-hold MR imaging of the liver with flexible contrast. *Radiology* **177,** 515–521 (1990).
2. D. J. Atkinson, R. R. Edelman, Cine angiography of the heart in a single breath hold with a segmented TurboFLASH sequence. *Radiology* **178,** 357–360 (1991).
3. R. R. Edelman, W. J. Manning, E. Gervino, W. Li, Flow velocity Quantification in human coronary arteries with fast, breath-hold MR angiography. *JMRI* **3,** 699–703 (1993).
4. J. Keegan, D. Firmin, P. Gatehouse, D. Longmore, The application of breath hold phase velocity mapping techniques to the measurement of coronary artery blood flow velocity: phantom data and initial *in vivo* results. *Magn. Reson. Med.* **31,** 526–536 (1994).
5. H. Li, G. D. Clarke, M. NessAiver, H. Liu, R. Peshock, Magnetic resonance imaging k-space segmentation using phase-encoding groups: the accuracy of quantitative measurements of pulsatile flow. *Med. Phys.* **22,** 391–399 (1995).
6. T. K. F. Foo, M. A. Bernstein, A. M. Aisen, R. J. Hernandez, B. D. Collick, T. Bernstein, Improved ejection fraction and flow velocity estimates with use of view sharing and uniform repetition time excitation with fast cardiac techniques. *Radiology* **195,** 471–478 (1995).
7. R. Frayne, J. A. Polzin, Y. Mazaheri, T. M. Grist, C. A. Mistretta, Effect of and correction for in-plane motion on coronary flow measurements, *in* "Proc., SMR, Third Meeting, Nice, France, 1995," p. 563.
8. T. A. Spraggins. Wireless retrospective gating: applications to cine cardiac imaging. *Magn. Reson. Imaging* **8,** 675–681 (1990).
9. G. H. Glover, N. J. Pelc, A rapid-gated cine MRI technique. *in* "Magnetic Resonance Annual 1988" (H. Y. Kressel HY, Ed.), pp. 299–333, Raven, New York, 1988.
10. G. L. Nayler, D. N. Firmin, D. B. Longmore, Blood flow imaging by cine magnetic resonance. *J. Comput. Assist. Tomogr.* **10,** 715–722 (1986).
11. N. J. Pelc, R. J. Herfkens, A. Shimakawa, D. R. Enzmann, Phase contrast cine magnetic resonance imaging. *Magn. Reson. Quarterly* **7,** 229–254 (1991).
12. R. Frayne, B. K. Rutt, Frequency response of retrospectively gated phase-contrast MR imaging: effect of interpolation. *JMRI* **3,** 907–917 (1993).
13. N. J. Pelc, M. A. Bernstein, A. Shimakawa, G. H. Glover, Encoding strategies for three-dimensional phase-contrast MR imaging of flow. *JMRI* **1,** 405–413 (1991).
14. R. N. Bracewell, "The Fourier Transform and Its Applications," McGraw-Hill, New York, 1986.
15. W. W. Nichols, M. F. O'Rourke, "McDonald's Blood Flow in Arteries," Lea and Febiger, Philadelphia, 1990, p. 276.
16. R. Frayne, B. K. Rutt, Frequency response of prospectively gated phase-contrast MR velocity measurements. *JMRI* **5,** 65–73 (1995).
17. M. A. Bernstein, A. Shimakawa, N. J. Pelc, Minimizing TE in moment-nulled or flow-encoded two- and three-dimensional gradient-echo imaging. *JMRI* **2,** 583–588 (1992).
18. C. L. Dumoulin, S. P. Souza, R. D. Darrow, N. J. Pelc, W. J. Adams, S. A. Ash, Simultaneous acquisition of phase-contrast angiograms and stationary-tissue images with Hadamard encoding of flow-induced phase shifts. *JMRI* **1,** 399–404 (1991).
19. L. B. Jackson, "Digital Filters and Signal Processing," Kluwer Academic Publishers, Boston, 1989.
20. J. A. Polzin, F. R. Korosec, M. T. Alley, T. M. Grist, C. A. Mistretta, Peak flow measurements using a segmented 2D phase-contrast acquisition, *in* "Proc., SMR, Second Meeting, San Francisco, 1994," p. 989.
21. R. Frayne, D. W. Holdsworth, L. M. Gowman, D. W. Rickey, M. Drangova, A. Fenster, B. K. Rutt, Computer-controlled flow simulator for MR flow studies. *J. Magn. Reson. Imaging* **2,** 605–612 (1992).
22. W. H. Press, S. A. Teukolsky, W. T. Vetterling, B. P. Flannery, "Numerical Recipes in C: the Art of Scientific Computing," Cambridge University Press, Cambridge, 1992.
23. M. H. Buonocore, L. Gao, Experimental study of the effects of "fractional" gating on flow measurements. *Magn. Reson. Med.* **31,** 429–436 (1994).
24. E. M. Haacke, G. W. Lenz, A. D. Nelson, Pseudo-gating: elimination of periodic motion artifacts in magnetic resonance imaging without gating. *Magn. Reson. Med.* **4,** 162–174 (1987).